

Article

Thermal Cycling Test of Solar Salt in Contact with Sustainable Solid Particles for Concentrating Solar Power (CSP) Plants

Marc Majó , Adela Svobodova-Sedlackova, Ana Inés Fernández , Alejandro Calderón * 
and Camila Barreneche * 

Department of Materials Science and Physical Chemistry, Universitat de Barcelona, Martí I Franqués 1-11, 08028 Barcelona, Spain; marc.majo@ub.edu (M.M.); adela.svobodova@ub.edu (A.S.-S.); ana_inesfernandez@ub.edu (A.I.F.)

* Correspondence: acalderon@ub.edu (A.C.); c.barreneche@ub.edu (C.B.); Tel.: +34-934-021-317 (C.B.)

Abstract: Thermal energy storage (TES) is crucial in bridging the gap between energy demand and supply globally. Concentrated Solar Power (CSP) plants, employing molten salts for thermal storage, stand as an advanced TES technology. However, molten salts have drawbacks like corrosion, solidification at lower temperatures, and high costs. To overcome these limitations, research is focusing on alternative TES materials such as ceramic particles. These solids match molten salts in energy density and can withstand higher temperatures, making them well-suited for CSP systems. This study revolves around subjecting Solar Salt alone and Solar Salt alongside Volcanic Ash (VA) and Electric Arc Furnace Slag (EAFS) to a comprehensive thermal cycling test. This test is designed to assess the compatibility over the thermal cycles of the Solar Salt and the Solar Salt in contact with these solids in a CSP plant with a thermocline configuration. With a final thermal and chemical evaluation, our observations indicate that EAFS and VA demonstrate promising compatibility but an increase in the reduction rate of the Solar Salt due to a catalyst effect from EAFS in contact with the salt. No discernible alterations were detected in the properties of either the solid materials or solar salt when combined.

Keywords: CSP; TES; molten salts; solid particle storage; thermal cycling



Citation: Majó, M.; Svobodova-Sedlackova, A.; Fernández, A.I.; Calderón, A.; Barreneche, C. Thermal Cycling Test of Solar Salt in Contact with Sustainable Solid Particles for Concentrating Solar Power (CSP) Plants. *Energies* **2024**, *17*, 2349. <https://doi.org/10.3390/en17102349>

Academic Editor: Antonio Rosato

Received: 25 March 2024

Revised: 22 April 2024

Accepted: 11 May 2024

Published: 13 May 2024



Copyright: © 2024 by the authors. Licensee MDPI, Basel, Switzerland. This article is an open access article distributed under the terms and conditions of the Creative Commons Attribution (CC BY) license (<https://creativecommons.org/licenses/by/4.0/>).

1. Introduction

Thermal energy storage (TES) stands as a promising solution for the global energy challenge of bridging the gap between energy demand and supply. Utilizing TES enables the storage of surplus clean energy produced during low-demand periods, like sun-rich daylight hours, for subsequent release during high-demand periods, such as nighttime or cloudy intervals [1]. As outlined by the International Energy Agency [2], TES offers a cost-effective means to integrate renewable energy sources like solar and wind power into the grid. It concurrently enhances grid reliability and stability. Moreover, TES contributes to reducing greenhouse gas emissions by minimizing reliance on fossil fuel-driven thermal power plants to meet peak demand [3].

A solar power generation technology known as concentration solar power (CSP) tower plants with molten salt-based energy storage systems concentrate solar energy using heliostat mirrors to heat a heat transfer fluid (HTF), generating electricity through a heat exchanger. This technology stores heat in molten salts, like solar salt (a mix of sodium nitrate and potassium nitrate) which is the most common HTF used in CSP plants, allowing continued electricity production after sunset, preventing energy dips. Notable plants, like Crescent Dunes in Nevada and Gemasolar in Seville, have 10 to 15 h of thermal storage. This technology is established globally, with ongoing projects in various countries like China, the UAE, Morocco, South Africa, the US, and Chile, with expectations for more tower CSP plants and diverse solar power projects in the near future [4–8].

Solar salt, while offering dispatchable power and favorable thermal qualities for Concentration Solar Power (CSP) reactors, has drawbacks to consider. Its corrosiveness to certain metals and solidification at around 230 °C bring risks to system components and fluid circulation. Despite being widely used in commercial solar plants, the first reaction that could lead to decomposition starts around 400 °C. This equilibrium reaction in the presence of oxygen, will lead to a reduction of the nitrate salt impacting in its performance and altering its properties [9,10].

Ceramic beads and similar solid particles have emerged as a potential thermal energy storage solution for Concentration Solar Power (CSP) plants [11]. They have a high thermal energy storage density, comparable with molten salts, and exhibit resilience against higher temperatures, making them suitable for integration into CSP systems. However, despite their advantages, sensible solid thermal energy storage systems possess a drawback of relatively lower energy density in terms of kWh/m³ compared to other liquid or latent and thermochemical methods. Despite this limitation, they remain the more advanced and commercially developed options [12].

Utilizing alternative materials, like natural materials, waste, or by-products, in thermal energy storage aligns with the principles of the circular economy and its integration into future energy systems [13]. Applying these materials for thermal energy storage repurposes them, preventing their disposal as waste. Industrial waste heat or solar heat from concentrated solar plants exemplify sources where heat can be captured and stored in various systems, such as molten salt, phase change materials, or sensible heat storage technologies. This stored energy can later generate electricity or heat, reducing reliance on traditional energy sources and lowering greenhouse gas emissions from industrial processes.

This study aims to assess the compatibility between Solar Salt and two different solid particle materials using a thermal cycling test. The thermal cycle will range between 250 °C and 550 °C to simulate the thermal stress and exposure that Solar Salt and the particles would experience in a CSP system utilizing a solid particle packed bed as a TES system. This assessment will be fundamental in evaluating the viability of the solids and their compatibility with Solar Salt in this context.

2. Materials and Methods

2.1. Materials

The Solar Salt mixture comprises sodium nitrate and potassium nitrate in a ratio of 60:40 by weight. Each component was sourced from Merck ACS reagent grade, with a purity exceeding 99.0%. The compounds exhibit minimal impurities: sulfate (<0.003%), calcium (<0.005%), nitrite (<0.001%), sodium (<0.005%), and magnesium (<0.002%). The solid particle materials investigated in this study comprise an Electric Arc Furnace Slag (EAFS) obtained from Celsa Group, a by-product from the steel industry. Additionally, Volcanic Ash (VA) sourced from the 2021 eruption in La Palma, Canary Islands, Spain, was included. This natural material was collected near El Paso village along the western flank of La Palma island's Cumbre Vieja rift zone. The VA samples were provided by members of the Institute for Environmental Studies and Natural Resources (I-UNAT) at the University of Las Palmas de Gran Canaria. The materials received, presented in Figure 1, were sieved to a maximum size of 600 µm.

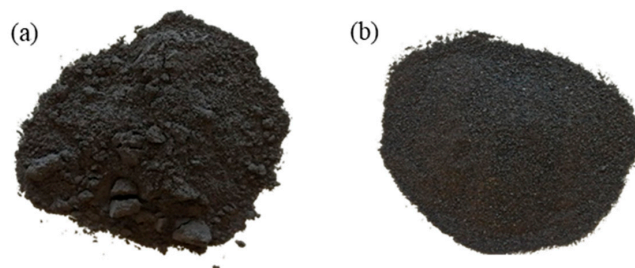


Figure 1. Images of (a) electric arc furnace slag (EAFS) and (b) volcanic ash (VA) as received.

2.2. Methodology: Cycling Test

The evaluation of the samples was carried out in a high-temperature programmable furnace capable of controlling the heating rate. Since the cooling cannot be controlled by the device, manual convection was necessary to quickly cool the sample, recreating operational conditions when a cold HTF will extract the heat of the TES material. This was achieved by opening the furnace door, creating induced convection. The temperature range was from 250 °C to 550 °C, with a heating rate of 5 °C/min for heating and 15 °C/min for induced cooling. A complete cycle could be conducted in approximately 1 h and 20 min. A total of 100 cycles were completed, after which the materials were separated by dissolving the salt in water and filtering it with a cellulose filter paper with a pore diameter of 11 µm and a thickness of 180 µm. Subsequently, the three solar salt samples were evaluated and compared to a non-treated salt, as well as the two solid materials. The temperature profile followed during the cycling test is depicted in Figure 2.

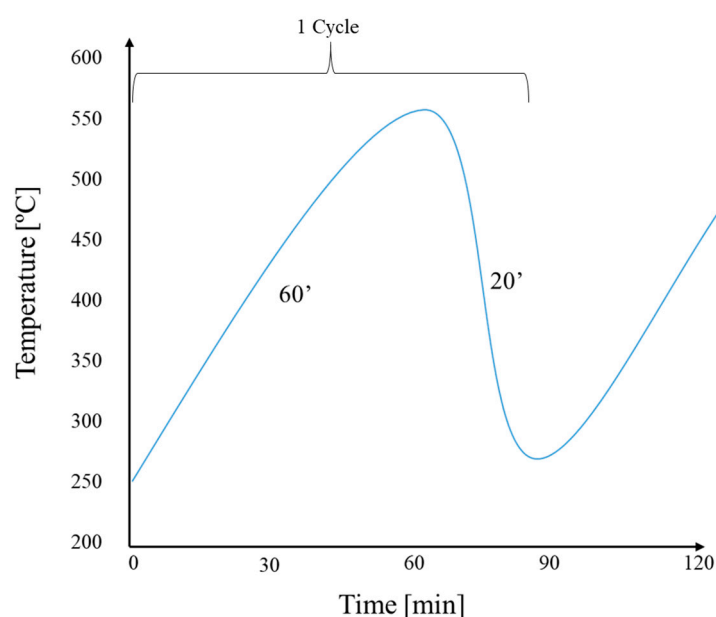


Figure 2. Temperature profile versus time of the cycling program conducted to the samples of solar salt in contact with the materials.

2.3. Characterization Techniques

2.3.1. Chemical Evaluation

The Solar Salt was initially isolated from the solid particle material and subsequently analyzed using X-ray powder diffraction (XRD) equipment from PANalytical (Malvern Panalytical, X'Pert PRO MPD, Madrid, Spain). A comparative analysis was conducted on the Solar Salt before and after thermal cycling, as well as on the Solar Salt that had previously interacted with the solid particles. To assess the degradation process of the Solar Salt, quantification of NO_2^- formation from the initial NO_3^- salt was performed. This involved utilizing XRD evaluation software (X'Pert HighScore version 2.2.3 PANalytical B. V.) to compare the initial NO_3^- peaks with the newly obtained NO_2^- peaks.

2.3.2. Thermal Evaluation

Thermal characterization was conducted utilizing a Differential Scanning Calorimeter (Mettler Toledo, DSC 822 3+, Barcelona, Spain). Following the area approach outlined by Ferrer et al. [14], the specific heat capacity of all samples was calculated. Three measurement repetitions were carried out under an N_2 atmosphere with a flow rate of 50 mL/min at 400 °C. Furthermore, an assessment of the melting point and enthalpy of fusion for all Solar Salt samples was conducted.

Additionally, a thermogravimetric analysis (TGA) of the solids was executed up to 600 °C in an air atmosphere. The analysis employed a Q600 SDT apparatus from TA Instruments, employing a heating ramp of 10 °C/min.

2.3.3. Physical Evaluation

The surface morphology and average size of the solid particle materials were investigated using a Scanning Electron Microscope (SEM, Hitachi TM3030, Hitachinaka, Japan). This analysis conducted both pre- and post-thermal cycling, aims to identify any structural alterations induced by thermal stresses.

Moreover, a comprehensive evaluation of particle size distribution (PSD) in the solid materials was performed utilizing a Beckman Coulter LSTM 13 320 laser diffraction particle size analyzer. The obtained data were subjected to analysis employing the Fraunhofer mathematical model, specifically tailored for opaque particles larger than 30 µm in size.

3. Results and Discussion

3.1. Evaluation of Solar Salt Samples

The chemical evaluation of Solar Salt samples is presented with a comparison of XRD patterns for molten salts post-thermal treatment and indicates a potential elevation in nitrite levels within solar salt in contact with the EAFS by-product. In Figure 3, the diffractogram for the Solar Salt/EAFS sample exhibits distinct peaks at 30°, 32°, and 44°, aligning with the presence of nitrite. Notably, the peak list for NaNO₂ confirms heightened intensity specifically at 30°. The main peaks are indicated by blue arrows in Figure 3.

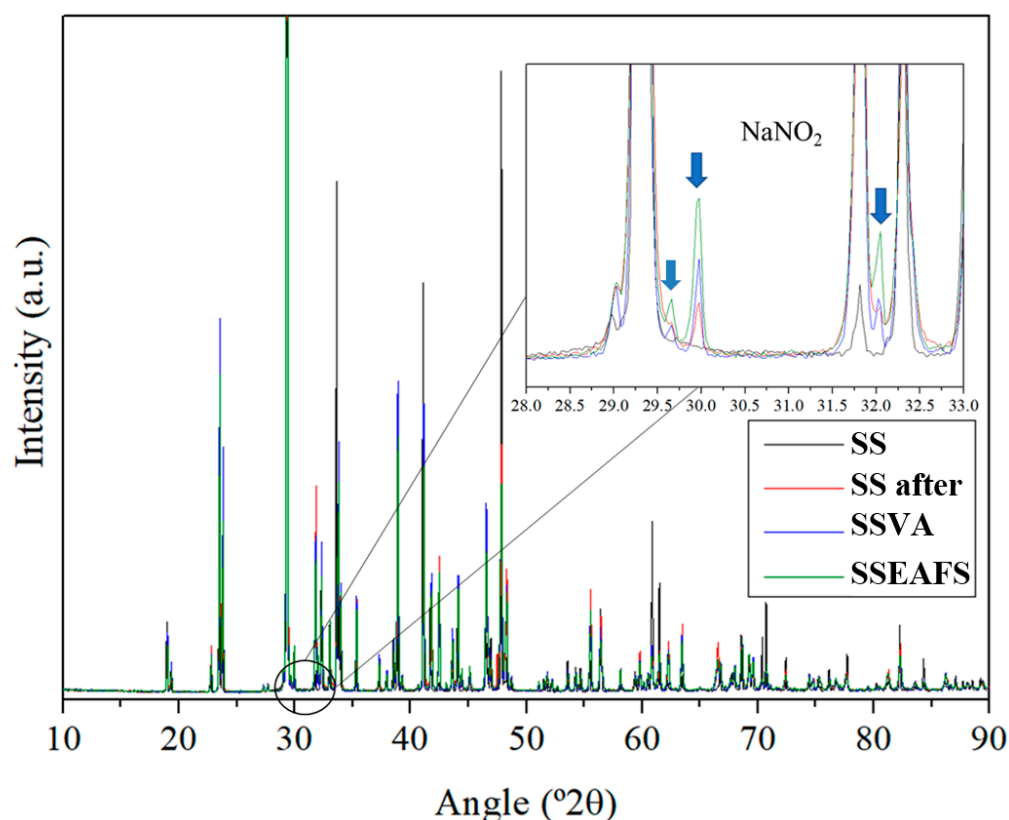


Figure 3. XRD peaks comparison of Solar Salt (SS) samples before and after thermal cycling alone (SS after) and in contact with the solid particles of Volcanic Ash (SSVA) and steel slag (SSEAFS).

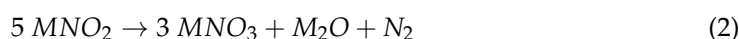
A quantification of the nitrite content was conducted on all cycled Solar Salt samples, and the results were compared with the XRD diffractogram evaluation. The quantification was performed using the obtained diffractograms and an evaluation software.

The natural reduction from nitrate to nitrite occurs under typical conditions of temperature and atmosphere. In the presence of oxygen, this reduction continues until an equilibrium ratio between nitrite/nitrate is achieved [10]. Table 1 indicates that Solar Salt samples in contact with the solids, SSVA and SSEAFS, exhibited higher nitrite formation compared to the Solar Salt sample cycled alone. As the conditions and masses were equal for all samples, it can be inferred that these materials functioned as catalysts in nitrite formation. The higher presence of iron oxides in the sample, notably more pronounced in the EAFS sample, could likely be the cause.

Table 1. Nitrite content calculated from XRD patterns from the Solar Salt samples after the thermal cycling test.

Sample	Nitrite Content (wt.%)
SS after	1.18
SS VA	2.04
SS EAFS	4.35

Monitoring nitrite formation over time is crucial as it could signify the initial stage of potential salt degradation, as described in Equations (1) and (2) where: “M” indicates Na or K.



The first reaction occurs at temperatures below 400 °C, leading to nitrite production, which does not significantly impact the mixture’s properties. The second reaction is considered the true degradation process of the salt due to the corrosive nature of alkaline oxides [9].

The thermal evaluation results of the Solar Salt samples are detailed in Table 2. All thermal properties (specific heat capacity, enthalpy of fusion, and melting point) exhibit a reduction in line with the increasing nitrite content in the samples. This correlation aligns with the characteristics of nitrite salts, known for their lower enthalpy of fusion and reduced melting points. These findings corroborate the prior observations from XRD patterns, indicating no chemical alterations in the salt when in contact with the solids.

Table 2. Thermal properties evaluated and compared with Solar Salt mixture with no treatment and the variation of the properties before and after the thermal cycling.

	Solar Salt	SS after	SS VA	SS EAFS
C_p (400 °C) [J/g·°C]	1.48 ± 0.01	1.46 ± 0.01	1.38 ± 0.01	1.40 ± 0.01
ΔH_{fus} [J/g]	106.1 ± 0.1	104.8 ± 0.1	97.8 ± 0.1	87.1 ± 0.1
T_m [°C]	222.8 ± 0.2	219.9 ± 0.2	219.1 ± 0.3	212.5 ± 0.2
C_p variation after cycling [J/g·°C]		−0.02 ± 0.01	−0.10 ± 0.01	−0.08 ± 0.01
ΔH_{fus} variation after cycling [J/g]		−1.3 ± 0.1	−8.3 ± 0.1	−19.0 ± 0.1
T_m variation after cycling [°C]		−2.9 ± 0.2	−3.7 ± 0.3	−10.3 ± 0.2

3.2. Evaluation of Solid Particles Samples

The SEM images before and after thermal cycling, illustrated in Figure 4 for each solid, depict the morphology, roughness, and stability of the materials towards the thermal shock. In Figure 4a, describing EAFS, larger particles with smooth surfaces are surrounded by smaller particles adhering to their surfaces. Post-cycling, the appearance remains similar, characterized by numerous small particles attached to the larger ones.

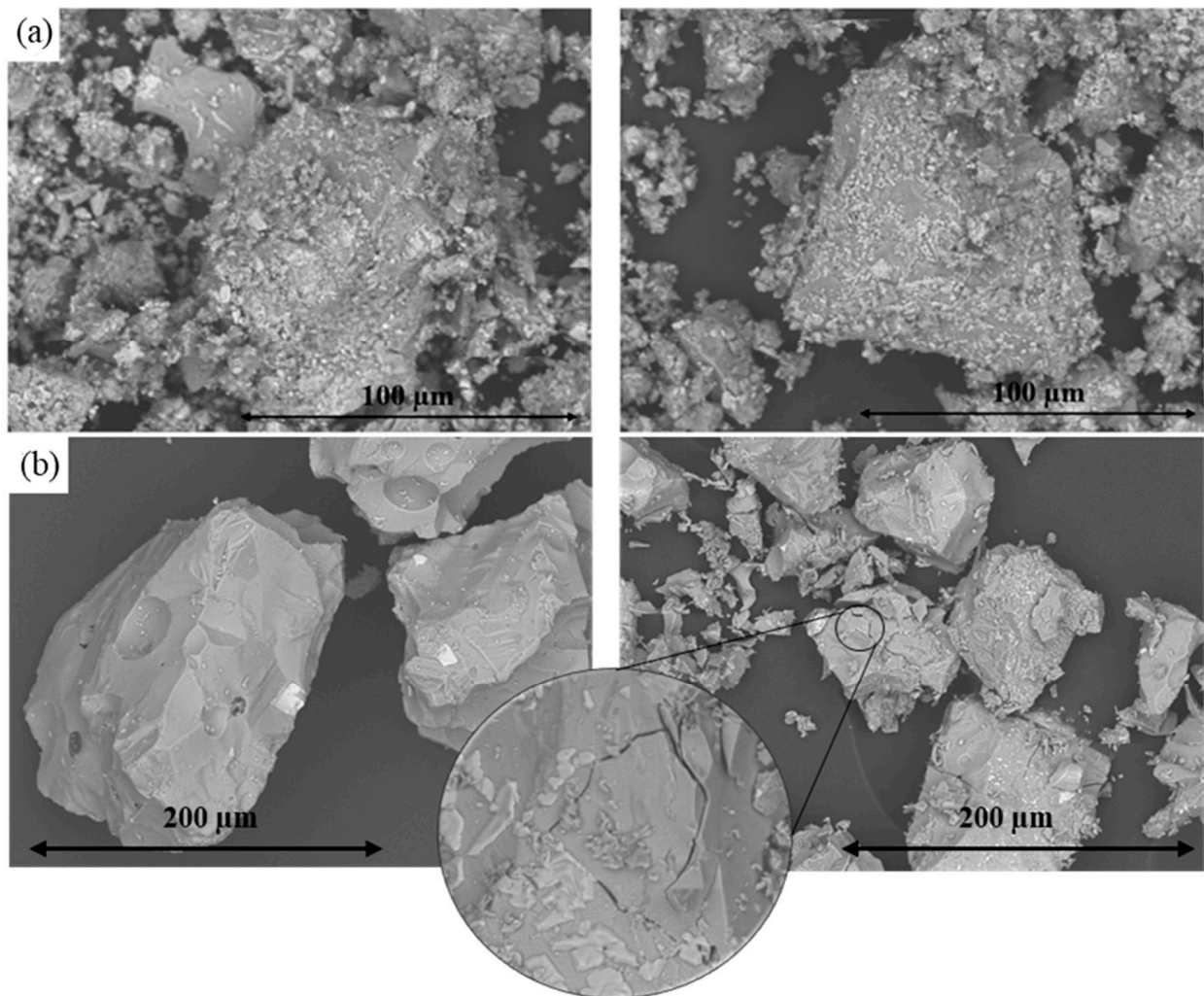


Figure 4. SEM images of (a) EAFS and (b) VA particles after (left) and before (right) thermal cycling treatment. Also, an amplification of a cracked area in VA after cycling.

Conversely, Figure 4b displays the VA particles with noticeably smoother surfaces, featuring minor inclusions and some slits. After treatment, smaller particles appear attached to the surfaces of larger ones, and multiple cracks have developed in several larger particles. The thermal shock likely resulted in the breakage of some particles, leading to the generation of fines in the VA sample. The presence of fine particles and the breakage of larger particles will affect the packing of the bed, thereby modifying the requirements for the Heat Transfer Fluid (HTF) to flow correctly through the bed. This can lead to an increase in pressure drop and other fluid mechanical considerations. While small particles may enhance thermal efficiency, this must be balanced to ensure that the HTF is not adversely affected, maintaining overall performance.

The results of the thermal evaluation of VA and EAFS particles are presented in Table 3, showing variations in heat capacity and thermal stability observed through mass loss during the initial exposure at 600 °C and subsequent exposure at the same temperature in a prior cycling assessment.

Table 3. Specific heat capacity (C_p) at 400 °C and mass loss of the materials tested as received and before the cycling test.

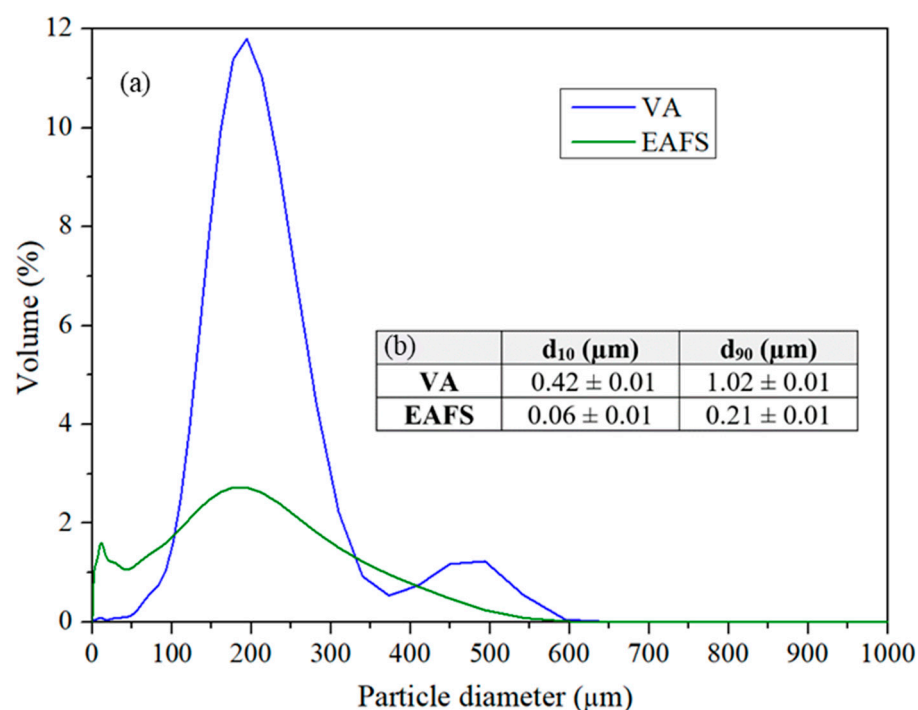
	C_p (400 °C) [J/g·°C]	Mass Loss (%) First Exposition at 600 °C	Mass Loss (%) Second Exposition at 600 °C
VA initial	1.07 ± 0.01	0.57	0.02
VA after	1.04 ± 0.01	-	-
EAFS initial	0.91 ± 0.01	−4.36	−0.09
EAFS after	0.94 ± 0.01	-	-

The heat capacity of both samples shows a slight change but nothing significant. However, in the previous thermal stability evaluation, a mass gain is noticeable in VA samples. This gain coincided with a color change from black to reddish, potentially indicating oxidation of the iron compounds present in the sample. The material remained stable during the second pre-test in the thermogravimetric evaluation.

In contrast, EAFS experienced continuous mass loss across all temperatures. This mass loss does not exhibit a precise degradation phenomenon as it's not clearly evident in the thermogravimetric evaluation. Nevertheless, subsequent cycles showed greater stability with only a slight mass change.

In summary, the solids have exhibited an excellent thermal stability within the temperature range. Nonetheless, it's recommended to consider a pretreatment to fully inert the materials before their contact with molten salts.

The particle size distribution of the samples is depicted in Figure 5, showing the results in (a) volume percentage concerning the entire sample and (b) the d_{10} and d_{90} values, that indicate the sizes at which 10% and 90% of the particles are smaller than the indicated value, respectively.

**Figure 5.** Particle size distribution of VA and EAFS samples represented in (a) volume percentage from the total and (b) d_{10} and d_{90} numbers that express that 10% and 90% of the particles have a size lower than the value.

The assessment based on volume percentage demonstrates that the VA sample contains larger particles compared to EAFS. Nonetheless, both materials exhibit a considerable number of very small particles. For a maximum and uniform packing of the solids, a uniform gradation is necessary. An optimal void reduction and maximum material packing, a precise and uniform size distribution is essential [15]. Additionally, minimizing the excessive presence of fine particles is crucial to prevent mechanical issues within the fluid flow through the bed. This precaution is necessary as it could otherwise lead to increased fluid pressure drop [16].

4. Conclusions

The development and completion of an automated cycling device capable of rapidly thermally cycle liquid and solid samples have been achieved. Initial cycling trials involving 100 cycles with Solar Salt and Solar Salt in the presence of two different solids have been successfully conducted.

Evaluation of the cycled Solar Salt samples indicates no observable chemical changes in the composition. However, the presence of EAFS particles has shown a catalyst effect on the equilibrium between sodium nitrate and sodium nitrite reactions. This presence of nitrites has altered the thermal properties of Solar Salt, suggesting that solid particle materials might influence the equilibrium of Solar Salt but not chemically.

Thermal assessment of the solid particles revealed some cracks in larger VA particles due to high thermal shock, whereas the EAFS particles remained stable. Nevertheless, the abundance of fine particles in both materials could potentially affect operations due to fluid mechanics issues, emphasizing the importance of a well-graded particle size distribution.

In summary, the potential for utilizing low-cost solid particle materials in packed bed tanks appears promising. By employing an appropriate particle size distribution to enhance packing and reduce void fraction, these solids have demonstrated usefulness in contact with molten salts and potentially other fluids. Considering their composition and thermal stability, exploring the utilization of these solids at higher temperatures with other fluids warrants further study.

Author Contributions: A.C., C.B. and A.I.F. contributed in the conceptualization, methodology and supervision. M.M. contributed in the writing of the original draft, data curation, methodology and writing review and editing, A.S.-S. contributed in data curation, methodology and writing review and editing. Also, C.B. and A.I.F. contributed with project administration and funding acquisition. All authors have read and agreed to the published version of the manuscript.

Funding: This research received no external funding.

Data Availability Statement: The original contributions presented in the study are included in the article, further inquiries can be directed to the corresponding author/s.

Acknowledgments: This work is part of PCI2020-120695-2 and PCI2020-120682-2 projects funded by Ministerio de Ciencia e Innovación—Agencia Estatal de Investigación (MCIN/AEI/10.13039/501100011033) and by the European Union “NextGenerationEU”/PRTR”, Development and evaluation of novel concepts for LHTES funded by CSO—Israeli Ministry of Energy, 120N663 project funded by TÜBITAK—Scientific and Technological Research Council of Turkey, and 121N737 project funded by TÜBITAK. The authors would like to thank the Catalan Government for the quality accreditation given to their research group DIOPMA (2017 SGR 0118, 2021 SGR 00708). DIOPMA is a certified agent TECNIO in the category of technology developers from the Government of Catalonia.

Conflicts of Interest: The authors declare no conflicts of interest.

References

1. Alva, G.; Lin, Y.; Fang, G. An overview of thermal energy storage systems. *Energy* **2018**, *144*, 341–378. [CrossRef]
2. Publications, I.E. World Energy Outlook 2022, Int. Energy Agency. 2022. Available online: <https://www.iea.org/reports/world-energy-outlook-2022> (accessed on 10 May 2024).
3. Gunasekara, S.N.; Barreneche, C.; In, A.; Calder, A.; Ravotti, R.; Risti, A.; Weinberger, P.; Paksoy, H.Ö.; Koçak, B.; Rathgeber, C.; et al. Thermal Energy Storage Materials (TESMs)—What Does It Take to Make Them Fly? *Crystals* **2021**, *11*, 1276. [CrossRef]

4. Calderón, A.; Barreneche, C.; Prieto, C.; Segarra, M. Concentrating Solar Power technologies: Bibliometric study of past, present and future trends in CSP research. *Front. Mech. Eng.* **2021**, *7*, 682592. [[CrossRef](#)]
5. Bauer, T.; Odenthal, C.; Bonk, A. Molten Salt Storage for Power Generation. *Chemie-Ingenieur-Technik* **2021**, *93*, 534–546. [[CrossRef](#)]
6. Tehrani, S.S.M.; Taylor, R.A.; Nithyanandam, K.; Ghazani, A.S. Annual comparative performance and cost analysis of high temperature, sensible thermal energy storage systems integrated with a concentrated solar power plant. *Sol. Energy* **2017**, *153*, 153–172. [[CrossRef](#)]
7. Bauer, T.; Pflieger, N.; Breidenbach, N.; Eck, M.; Laing, D.; Kaesche, S. Material aspects of Solar Salt for sensible heat storage. *Appl. Energy* **2013**, *111*, 1114–1119. [[CrossRef](#)]
8. NREL, S.P. CSP Projects Around the World, Iea, Energy Technol. Netw. 2023. Available online: <https://www.solarpaces.org/csp-technologies/csp-projects-around-the-world/> (accessed on 20 June 2023).
9. Delise, T.; Tizzoni, A.C.; Ferrara, M.; Corsaro, N.; D'Ottavi, C.; Sau, S.; Licocchia, S. Thermophysical, environmental, and compatibility properties of nitrate and nitrite containing molten salts for medium temperature CSP applications: A critical review. *J. Eur. Ceram. Soc.* **2019**, *39*, 92–99. [[CrossRef](#)]
10. Villada, C.; Bonk, A.; Bauer, T.; Bolívar, F. High-temperature stability of nitrate/nitrite molten salt mixtures under different atmospheres. *Appl. Energy* **2018**, *226*, 107–115. [[CrossRef](#)]
11. Calderón, A.; Palacios, A.; Barreneche, C.; Segarra, M.; Prieto, C.; Rodríguez-Sánchez, A.; Fernández, A.I. High temperature systems using solid particles as TES and HTF material: A review. *Appl. Energy* **2018**, *213*, 100–111. [[CrossRef](#)]
12. Gutierrez, A.; Miró, L.; Gil, A.; Rodríguez-aseguinolaza, J.; Barreneche, C.; Calvet, N.; Py, X.; Fernández, A.I.; Grágeda, M.; Ushak, S.; et al. Advances in the valorization of waste and by-product materials as thermal energy storage (TES) materials. *Renew. Sustain. Energy Rev.* **2016**, *59*, 763–783. [[CrossRef](#)]
13. Society, E.M.R. Materials Innovation for the Global Circular Economy and Sustainable Society, VI World Mater. Summit. 2017. Available online: https://www.esf.org/fileadmin/user_upload/esf/2018_WMS_online.pdf (accessed on 10 May 2024).
14. Ferrer, G.; Barreneche, C.; Solé, A.; Martorell, I.; Cabeza, L.F. New proposed methodology for specific heat capacity determination of materials for thermal energy storage (TES) by DSC. *J. Energy Storage* **2017**, *11*, 1–6. [[CrossRef](#)]
15. Zhang, S.; Liu, W.; Granata, G. Effects of grain size gradation on the porosity of packed heap leach beds. *Hydrometallurgy* **2018**, *179*, 238–244. [[CrossRef](#)]
16. Allen, K.G.; von Backström, T.W.; Kröger, D.G. Packed bed pressure drop dependence on particle shape, size distribution, packing arrangement and roughness. *Powder Technol.* **2013**, *246*, 590–600. [[CrossRef](#)]

Disclaimer/Publisher's Note: The statements, opinions and data contained in all publications are solely those of the individual author(s) and contributor(s) and not of MDPI and/or the editor(s). MDPI and/or the editor(s) disclaim responsibility for any injury to people or property resulting from any ideas, methods, instructions or products referred to in the content.